A comparative analysis of the folding and misfolding pathways of the third PDZ domain of PSD95 investigated under different pH conditions

Javier Murciano-Calles, Eva S. Cobos, Pedro L. Mateo, Ana Camara-Artigas, Jose C. Martinez

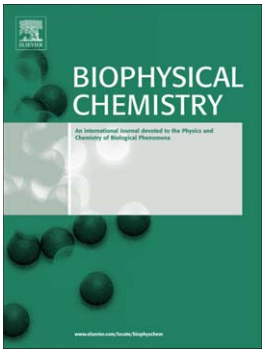

A comparative analysis of the folding and misfolding pathways of the third PDZ domain of PSD95 investigated under different pH conditions

Javier Murciano-Calles, Eva S. Cobos, Pedro L. Mateo, Ana Camara-Artigas, Jose C. Martinez

PII: S0301-4622(11)00186-4
DOI: doi: 10.1016/j.bpc.2011.05.018
Reference: BIOCHE 5529

To appear in: *Biophysical Chemistry*

Received date: 11 April 2011
Revised date: 20 May 2011
Accepted date: 21 May 2011

Please cite this article as: Javier Murciano-Calles, Eva S. Cobos, Pedro L. Mateo, Ana Camara-Artigas, Jose C. Martinez, A comparative analysis of the folding and misfolding pathways of the third PDZ domain of PSD95 investigated under different pH conditions, *Biophysical Chemistry* (2011), doi: 10.1016/j.bpc.2011.05.018

A comparative analysis of the folding and misfolding pathways of the third PDZ domain of PSD95 investigated under different pH conditions

Javier Murciano-Calles[†], Eva S. Cobos[†], Pedro L Mateo[†], Ana Camara-Artigas[‡] and Jose C. Martinez[†*]

[†] Department of Physical Chemisry and Institute of Biotechnology, Faculty of Sciences, University of Granada, 18071 Granada, Spain.

[‡] Department of Physical Chemistry, Biochemistry and Inorganic Chemistry, Faculty of Experimental Sciences, 04120 Almeria, Spain.

[*]Corresponding author:
Jose C. Martinez
Department of Physical Chemistry
Faculty of Sciences
University of Granada
18071- Granada, Spain
Tel: +34 958 242370
Fax: +34 958 272879
E-mail: jcmh@ugr.es

Abstract

Equilibrium unfolding at neutral pH of the third PDZ domain of PSD95 is well described by the presence of a partly unfolded intermediate that presents association phenomena. After some days' incubation annular and fibrillar structures form from the oligomers. At pH values below 3, however, differential scanning calorimetry shows that PDZ3 seems to unfold under a two-state scheme. Kinetic measurements followed by dynamic light scattering, ThT and ANS fluorescence reveal that the misfolding pathway still exists despite the absence of any populated intermediates and shows an irreversible assembling of the supramacromolecular structures as well as an appreciable lag-phase, contrary to what is found in similar experiments at neutral pH. Moreover, as shown by transmission-electron-microscopy images, the annular structures seen at neutral pH completely disappear from incubated solutions. According to the structural information, this titration behavior appears to be the consequence of a conformational equilibrium that depends on the protonation of some Glu residues located at the C-terminal α3 helix and at the hairpin formed by strands β2 and β3. Our calculations suggest that the enthalpic contribution of these interactions may well be as much as 40 kJ·mol^{-1}. The possible regulatory role of this equilibrium upon PDZ3 functionality and amyloid formation is briefly discussed.

Graphical Abstract
]Research Highlights
Unfolding at pH>3.5 of PSD95-PDZ3 reveals the presence of an equilibrium oligomeric intermediate state that self-associates into annular and fibrillar structures reversibly

At pH<3 PDZ3 seems to unfold under a two-state scheme, although the misfolding pathway still exists

The supramacromolecular structures organize irreversibly and show a lag-phase at acidic pH

This titration behavior is due to a conformational equilibrium that depends on the protonation of some Glu residues

The enthalpic contribution of these interactions may well be as much as 40 $kJ \cdot mol^{-1}$.

Keywords
folding intermediates; protein thermodynamics and stability; PDZ domains; oligomerization processes; annular/spherical aggregates; amyloid fibrils.

Abbreviations
DSC, differential scanning calorimetry; DLS, dynamic light scattering; CD, circular dichroism; TEM, transmission electron microscopy; PSD95, post-synaptic density-95 protein; PDZ, post-synaptic density-95 protein, disk-large tumor suppressor protein, zonnula occludens-1; PSD95-PDZ3 or PDZ3, third PDZ domain of PSD95 protein; SH3, Src-homology 3 domain; MAGUK, membrane-associated guanilate kinase; ThT, thioflavine T; ANS, 1-anilino-naphtalene-8-sulfonic acid.

1. Introduction

Protein aggregation is considered today to be a generic property of polypeptides and is thus a considerable problem for living organisms, which must develop response strategies to avoid its harmful effects. These effects span from arthritis to serious neurodegenerative diseases. At the molecular and energetic level, the self-organization mechanism of proteins relies on many properties related to both the protein system (hydrophobicity, β-sheet propensities etc.) and the solvent conditions (pH, ionic strength, organic reagents etc.). These properties can modulate the misfolding pathway in ways ranging from downhill to nucleation-cooperative aggregation mechanisms.

In spite of extensive reports in the literature, our knowledge of the basic processes by which polypeptide chains can give rise to well ordered supramacromolecular structures is still poorly understood [1]. It has been suggested that the concepts underlying protein aggregation might be similar to those describing the organization of synthetic polymers, which may explain some features of the growth-kinetic processes [2]. A recent study has put forward a general unifying mechanism based on the formulation of master equations that describe the kinetics of fibrillar self-assembling as resulting from three basic processes: i) a nucleation-dependent polymerization reaction (lag-phase), usually slower than the ii) elongation of pre-existing nuclei, and finally iii) a secondary nucleation event deriving from the fragmentation of fibrils [3].

The almost universal irreversibility of amyloid-growth processes has precluded any deeper understanding of them than their purely kinetic features, and so little is known about the dynamics and nature of the ensemble of states, the structural and energetic aspects of the organization of their supramacromolecular assemblies or even of the inter-conversion between their various types. In a previous work [4] we explored the misfolding pathway of the third PDZ domain of the PSD95 neuronal protein (PDZ3), comprising residues 302 to 402 of PSD95. At neutral pH at 60-70 ºC in plain water-buffered solutions the PDZ3 domain populates a trimeric β-sheet-rich intermediate state that leads to a stepwise and reversible formation of annular and protofibrillar structures, which remain in solution for various days and finally give rise to fibrils. Some authors have suggested that it is these annular and protofibrillar aggregates that are the toxic agents responsible for amyloid diseases, most probably through membrane interactions by pore formation [5,6].

To arrive at some insight into the molecular aspects of the misfolding pathway of PDZ3 we undertook DSC experiments under different pH conditions ranging from acidic to neutral. Surprisingly, the domain unfolded under a simple two-state scheme at pH values below 3, whereas the previously described three-state regime appeared above this value. Kinetic measurements followed by DLS, ThT and ANS fluorescence revealed that the misfolding pathway still existed despite the absence of any populated intermediates and showed an irreversible assembling of the supramacromolecular structures as well as an appreciable lag-phase at pH ≤ 3, contrary to what was found in respective experiments at neutral pH. Moreover, as shown by TEM images, the annular structures seen at neutral pH completely disappeared from incubated solutions.

This titration behavior might be attributed to the protonation equilibria of Glu and/or Asp residues, the pKa values of which are the only ones within the range of pH 3-4. An analysis of two 1.4 Å X-ray structures of PDZ3 reveals that some Glu residues appear to be principally responsible for the attachment of the α3 helix to the whole PDZ3 structure through the β-hairpin formed by strands β2 and β3. In addition, we have already described the cyclation of the acidic residue D322 into a succinimide ring at the β-turn organizing this β-hairpin [7]. Thus, when these acidic residues titrate above pH 3 the proton release would generate some degree of electrostatic repulsion between their negative charges in the β2-β3 hairpin as well as between the Glu side-chains and the π-electron clouds of some aromatic

rings of the C-terminal α3 helix, which might contribute to a weakening of the attachment. It has been proposed that this α3 helix may be a regulatory element of the binding properties of PDZ3 [7,8].

2. Materials and Methods

The PDZ3 sequence cloned into pQE30 plasmid was generously donated by Drs. Jose Reina (Institute of Biomedical Research, IRB, Barcelona, Spain) and Luis Serrano (EMBL-CRG, Barcelona, Spain). Residues 302 to 402 (in PSD95 numbering) were subcloned into pBAT4 (EMBL Core Purification Facility) and expressed in *E. coli BL21/DE3* cells. PDZ3 can be obtained at a ratio of 15 mg per liter of LB culture and purified by Superdex-75 chromatography (GE-Pharmacia) in 50 mM K-phosphate, 150 mM KCl, at pH 7.5. The molecular mass was 11004 Da as determined by MALDI-TOF experiments carried out at the Centro de Instrumentacion Cientifica (CIC) services of the University of Granada. The extinction coeficient used was 2985 $cm^{-1} \cdot M^{-1}$, determined as described elsewhere [9].

DSC experiments were conducted in two VP-DSC instruments from Microcal INC., as described elsewere [10]. PDZ3 experimental conditions were 50 mM buffer (either phosphate at pH 7.5, acetate at pH 4.0 or glycine/HCl at pH 2.0-3.5). DLS, CD and ThT and ANS fluorescence experimental details can be obtained from previous references [4,11]. TEM images of amyloid fibrils were made at the CIC services of the University of Granada. 1 % uranyl acetate was used for staining.

The two-state non-linear curve fittings of DSC traces at acidic pH values were made on the basis of the equations reported elsewhere [10]. The established three-state model including an oligomeric intermediate used to fit DSC traces above pH 3 ($nN \rightleftharpoons I_n \rightleftharpoons nU$) has also been described previously by us [4]. Linear functions for the heat-capacity functions $C_{pN}(T)$, $C_{pI}(T)$ and $C_{pU}(T)$ were always used. The unfolding (and dissociation in the case of the three-state model) temperatures, enthalpies and heat capacity functions for every experiment were obtained from the respective fitting analyses. The error intervals were taken to be three times the fitting standard errors (99 % confidence). The fitting equations for both models are described in detail in the Supplementary Material.

3. Results

3.1. PDZ3 unfolds under an apparent two-state scheme at acidic pH

As we showed in a previous work [4], the thermal unfolding of PDZ3 at neutral pH reveals the presence of an oligomeric equilibrium intermediate that populates maximally at around 60-70 ºC. The DSC traces comprise two well separated unfolding transitions, which can be fully described by a three-state association-dissociation equilibrium model ($nN \rightleftharpoons I_n \rightleftharpoons nU$). We observed a similar behavior when we extended our experiments to buffered solutions at pH values >3.5 (Fig. 1). Nevertheless, at pH values ≤ 3 the biphasic behavior disappeared and showed just a single endotherm, which can be described by a two-state model ($N \rightleftharpoons U$; Fig. 1). The quality of the fittings is surprisingly good, as revealed by Figure 1 and by their R-square parameters (Table 1). In addition, the reversibility of the unfolding process increased dramatically from 60 % for the biphasic traces to 90 % for those below pH 3.

Nevertheless, this simple unfolding model does not seem to describe the whole unfolding behavior of PDZ3 at pH ≤ 3 since an increase in protein concentration above 5 $mg \cdot mL^{-1}$ produced a post-transition shoulder similar to that observed at pH 3.5 (Fig. 1). This feature should not appear in a pure two-state unfolding system, which has been described as being concentration independent [10,12]. Therefore, we can conclude that the intermediate state, although still being inherent to the unfolding pathway, is not populated at acidic pH values and low protein concentrations due to its energetic destabilization.

3.2. Evaluation of electrostatic contributions of acidic residues to the thermodynamic parameters of unfolding

The titration behavior observed in DSC experiments is certainly due to the protonation equilibria of Glu and/or Asp residues, the pKa values of which are the only ones within the range of pH 3-4 (see Discussion for further details). To evaluate the whole energetic contribution of the electrostatic balance of Glu and Asp residues we have represented the unfolding enthalpies as a function of their respective unfolding temperatures obtained under the various pH conditions (Fig. 2). The values deriving from two-state analysis (pH $\leq$ 3) correlate well with a linear dependency. Furthermore, they coincide well with the hypothetical value of 54 $J \cdot g^{-1}$ at 110 ºC, which, as postulated by some authors [12-16], represents a convergence value of the enthalpy functions of small globular proteins. The slope of this regression provides a value for the unfolding heat-capacity change of 5.6 $kJ \cdot K^{-1} \cdot mol^{-1}$, which is comparable to the values obtained for other proteins of similar size [12,15].

The enthalpy values obtained from three-state analysis (pH > 3) do not, however, fit any such linear dependency (Fig. 2). Thus, considering that at these pH values the most relevant energetic feature appears to be that related to the titration of Glu and Asp residues, we can conclude that the roughly 40 $kJ \cdot mol^{-1}$ discrepancy between the values above pH 3 and the linear dependency of the enthalpy values under most acidic pH conditions may well be related to the heat contribution of some repulsive electrostatic forces developed upon the proton release of Glu/Asp residues above pH 3.

Since the ionization enthalpy of roughly solvent-exposed carboxilic groups is usually close to zero, the relatively high heat effect detected may be put down to some conformational change within the N state deriving from the proton uptake, being this state more structured at acid pH than at neutral. Nevertheless, we could not detect any such change by far-UV CD spectra, which show no appreciable differences between pH 3 and pH 7.5 (Fig. S1).

An alternative explanation for the enthalpic differences may conceivably be the low reversibility of the unfolding curves at neutral pH, which is probably due to the irreversible conversion of a fraction of the oligomeric intermediates into higher-order aggregates. This small proportion of species might decrease the unfolding enthalpy due to the reduction of the soluble protein fraction and/or to the exothermal heat effect that usually accompanies aggregation. Nevertheless, this decrease would depend on heating rate and protein concentration, but as our results show no dependence on any of these parameters (data not shown; [4]), we choose to discard this explanation.

3.3. A different mechanism of PDZ3 fibril organization at acidic pH

As we have shown in a previous work [4], at pH 7.5 and 60-70 ºC the intermediate species of PDZ3 can develop a misfolding pathway that begins with the formation of trimers, which appear above 50 ºC. These trimers self-associated into 12 nm particles that grew within a few days into protofibrillar and annular assemblies and then into fibrillar aggregates. The sequence of equilibrium events is summarized in Figure 3.

DLS experiments carried out with PDZ3 at acidic pH revealed a stepwise misfolding reaction, differing in some important aspects from that described above. Thus, the heating from 25 ºC to 60 ºC of a 8 $mg \cdot mL^{-1}$ protein sample in 50 mM glycine/HCl buffer at pH 3 indicates that monomeric species remained in solution until the final temperature, coexisting with other particles of 4.7 nm, which appeared above 50 ºC and comprised as much as 10 % of the total mass (not shown). When the sample was incubated at 60 ºC as a function of time the picture summarized in Figure 4 was obtained. Basically, both species remained within the solution after 4h although the mass percentage of the 4.7 nm species increased to 40 %. It was after this time when monomers definitely disappeared from the protein solution and the 4.7 nm particles populated to a maximum. A further incubation of the samples for longer times

revealed that the 4.7 nm particles increased in size. It should be noted that at pH 7.5 the monomers disappeared and fully trimerized before 60 ºC was reached [4]. These trimers never appeared at pH 3 however (Fig. 3).

Long-term incubated samples of PDZ3 at 60 ºC and pH 3 were analyzed by TEM (Fig. 5). Some particules of a few nm appeared after 4 hours' incubation, which may be the 4.7 nm particles seen by DLS. After 1 day only fibrillar structures appeared and these became longer, more populated and thicker with time. No annular structures were found at all in any of the different preparations. The fibrils had a similar curly shape to those seen at neutral pH, although they grew faster when compared to those at pH 7.5. Competition with annular structures within the misfolding pathway at neutral pH prevented the fibrils from maturing due to the early formation of these structures, whereas at acidic pH fibrils grew exclusively at the expense of the precursory oligomers. In addition, the dilution and cooling down of the samples to 25 ºC did not destroy the fibrils at pH 3, as it did at pH 7.5, indicating that the misfolding processes were essentially irreversible. DLS experiments also confirmed the irreversibility of misfolding, since the distribution of the particles remained the same when incubation at 60 ºC was interrupted.

3.4. ANS and ThT fluorescence experiments reveal a lag-phase during fibril growth and confirm the irreversibility of misfolding at pH 3

Heating a sample of a 8 $mg \cdot mL^{-1}$ PDZ3 inside the fluorimeter from 25 to 60 ºC at pH 3 did not lead to fluorescence when ThT 12 μM was added, although there was a small amount in the presence of 20 μM ANS (Fig. S2). When both ThT and ANS samples were incubated at 60 ºC, the fluorescence emission recorded as a function of time displayed a sigmoid kinetic profile with a lag-phase of around 100 min, where the fluorescence remained minimal, although a substantial increase in the signal occurred afterwards (Fig. 6). These curves displayed no sigmoidal shape at neutral pH, at which we observed a substantial and practically concomitant increase in the fluorescence of ThT and ANS samples at the beginning of their incubation at 60 ºC, indicating an essentially non-cooperative growth [4]. The lag period of these curves is well accepted as being a nucleation stage during which non-fluorescent oligomeric species are formed prior to the fibrillar structures that will grow under a subsequent rapid, cooperative regime. This behavior is that which has most frequently been observed among the many amyloidogenic proteins studied to date [3,17-19].

The considerable difference in shape of the ThT and ANS profiles also argues in favor of a different mechanism for the misfolding pathway between neutral and acidic pH conditions for PDZ3. Thus, their increase in fluorescence after roughly 2 h indicates that the non-fluorescent species formed during this lag period (basically monomers and 4.7 nm particles) did not expose hydrophobic patches and did not show typical β-aggregation, as occured at neutral pH with the respective trimeric and 12 nm oligomers. Therefore, the molecular nature of the fibril nuclei formed under either pH condition is substantially different.

Surprisingly, at pH 3 the DLS experiments showed only the presence of monomers and 4.7 nm particles after 4 hours' incubation, which does not coincide with the 2-hour lag-phase observed in the fluorescence experiments carried out in the presence of ThT and ANS. The question that arises is, "What might the species responsible for the increase in fluorescence after the lag-phase be?" The explanation could be an internal structural arrangement of PDZ3 monomers and/or oligomers. This conformational change may give rise to the exposure of hydrophobic surfaces and to β-sheet-rich species that act as precursors to the fibrillar structures. This conformational change was not detected by far-UV CD, all the spectra collected at different incubation times being practically identical in shape and displaying a

minimum at 217 nm (indicative of β-strand arrangements), which increased in intensity concomitantly with incubation time (Fig. S1).

Finally, in addition to DLS and TEM evidence, the essentially irreversible formation of the supramacromolecular assemblies at acidic pH was proven by spectral analysis of samples cooled down to 25 ºC after various hours' incubation at 60 ºC. The fluorescence spectra remained unaltered in all the solutions (Fig. S2), whereas at neutral pH a hyperchromic effect appeared, due to the disaggregation of these assemblies into their constituent protein monomers [4].

4. Discussion

4.1. pH-dependent differential features upon folding and misfolding of PDZ3

In a previous paper we described the folding pathway of the PDZ3 domain from PSD95 protein at neutral pH [4]. It consists of a well organized, stepwise, reversible process in which a trimeric intermediate state, which maximally populates at 60-70 º C, may be the precursory ensemble of a misfolding pathway. During misfolding this oligomeric intermediate self-associates into 12 nm particles that, after some days, lead to annular and fibrillar supramacromolecular assemblies (Fig. 3).

In this work we have extended our experiments on PDZ3 folding to acidic pH conditions and found some significant differences. Thus, DSC experiments revealed that below pH 3 the PDZ3 domain apparently unfolds under a two-state regime as a consequence of an energetic destabilization of the intermediate state, which does not populate at any temperature. Nevertheless, the misfolding pathway still remains under these acidic pH values, since fibrillar assemblies appeared after 1-2 days incubation at 60 ºC.

The DLS results also showed considerable differences during the early stages of self-assembling processes under acidic and neutral pH conditions. Thus, particles of different sizes formed in PDZ3 prior to the growth of fibrils (Fig. 3). In addition, TEM imaging only revealed fibrillar assemblies at pH 3 and the ThT and ANS fluorescence kinetic experiments were sigmoidal (lag-phase) compared to the exponential shape at neutral pH (no lag-phase). Furthermore, the whole set of kinetic experiments clearly indicated the completely irreversible nature of the misfolding species at acidic pH, which also runs contrary to the reversibility of the misfolding pathway found at neutral pH.

4.2. A thermodynamic explanation of the irreversibility of PDZ3 misfolding at acidic pH

As has been previously demonstrated in some examples [4,20], the energetic character of self-assembling processes can be satisfactorily explained by thermodynamic criteria. The stability of PDZ3 at pH ≤ 3 was within the range of 15-25 $kJ \cdot mol^{-1}$ (Table 1), whereas we had previously estimated the stability of the PDZ3 misfolding assemblies to be 25 $kJ \cdot mol^{-1}$ [4]. Thus, the higher stability of the N-state (around 40 $kJ \cdot mol^{-1}$; Table 1) than that of the aggregates may well explain the reversibility of misfolding at neutral pH, while the misfolded structures are preferred under acidic pH conditions, where the fibrils are slightly more stable than the N-state itself. The fact that the aggregates assembled more quickly at pH 3 than under neutral pH conditions can be explained by the competition between fibrils and annular structures within the misfolding pathway at neutral pH, whereas at acidic pH the fibrils grew exclusively at the expense of the precursory oligomers.

4.3. Electrostatic forces are responsible for the differential folding behavior of PDZ3 at neutral and acidic pH

The relevant role of electrostatic interactions in the organization of amyloid fibrils has been described elsewhere [21-23]. Variations in pH can modulate the electrostatic balance between intra- and inter-molecular forces among protein molecules. The different behavior of fibril growth found in the kinetic experiments under neutral (non-sigmoidal) and acidic (sigmoidal) conditions must be a direct consequence of the different stabilities of the precursory intermediate state shown by DSC. Thus, the presence of a lag-phase at acidic pH suggests that the formation of oligomeric assemblies needs to reach a critical number/size prior to promoting further aggregation. At neutral pH this process is energetically favoured by the stable precursory intermediate state that already oligomerizes during heating from room temperature to 60 ºC [4]. A similar pH-dependent behavior has been observed in human-serum albumin fibrillation processes [23].

Kinetic experiments also showed that the lag-phase at pH 3 continued for approximately two hours, but DLS did not reveal the appearance during this time of any new particle to which we might attribute the increase in fluorescence observed. Thus, under such conditions, monomeric and 4.7 nm particles remained exclusively for roughly four hours (Fig. 4). In addition, the lack of ThT and ANS fluorescence of these particles suggests that they neither exposed hydrophobic patches (ANS) nor showed typical β-aggregation (ThT), as happened at neutral pH with the corresponding trimers and 12 nm particles (Fig. 3). These observations clearly suggest that the oligomeric species will display different structural arrangements at the two pH values. Following this reasoning, the increase in fluorescence after the lag-phase at pH 3 would be the consequence of a conformational change in the protein molecules prior to the assembling of the fibrils, but we could not detect this by CD spectrum analysis.

4.4. The 1.4 Å X-ray structures of PDZ3 reveal a cluster of Glu/Asp residues as being responsible for the energetic destabilization of the unfolding intermediate at acidic pH

According to our experimental evidence, PDZ3 retains the three-state regime described at neutral pH, characterized by the presence of an energetically stable intermediate state, down to pH values of 4.0-3.5 (Fig. 1), whereas at pH ≤ 3 the intermediate does not stabilize at any temperature. Judging by the heat effect of unfolding, the intermediate is much less structured than the native state and there is no evidence that it inherits any structural element from the native conformation, since it contains mostly β-structure. In this study we also show that there is at least one acidic group per monomer within the oligomer, the pKa value of such group falls below 4. At the same time there must exist other titrating acidic groups within the native conformation that modulate its stability when pH changes. These groups with low pKa values might differ or remain the same between both the native and the intermediate states.

The high-resolution X-ray structures of PDZ3 [PDB: 3I4W and 3K82 [7]] show that with only a few exceptions these residues are highly exposed to the solvent. Thus, some Glu residues appear to be involved in the attachment of the α3 helix to the whole PDZ3 structure. These residues, mainly E334 from strand β3, and E396 and E401 from helix α3, can interact by means of the aliphatic side-chains between them, these interactions being influenced by the aromatic rings of residues F337 from the β3 strand, and Y397 and F400 from the α3 helix (Fig. 7). Nevertheless, when Glu residues titrate above pH 3 (pKa = 3.0-3.5) the proton release should generate some degree of electrostatic repulsion between the negative charges of the Glu side-chains, where the π-electron clouds of the aromatic rings might also contribute to this energy balance to some degree [24-28]. This phenomenon gives rise to an opening of the C-terminal α3 helix and of the β2-β3 region, as has also been shown by NMR [29]. The α3 helix constitutes an additional structural element compared to other typical PDZ domains, which are characterized by six β-strands and just two α-helices and which has been described elsewhere as an allosteric regulatory element that may modulate the binding affinity of this PDZ3 domain [8].

Furthermore, the X-ray structures of the loop connecting the β2 and β3 strands, formed by residues G329-G335 (GGEDGEG), identify the presence of a succinimide residue at the position of D332 (Fig. 7), which is considered to be an intermediate step in the process of Asp isomerization and Asn deamidation in proteins. From a conformational point of view, this circular arrangement decreases loop flexibility and at the same time results in the loss of a negative charge from the Asp carboxil group [7]. Apart from these observations, the only relevant feature of the other acidic residues consists of a salt-bridge formed by residues R312-D357, which probably does not enter into the energetic modulation between the different pH conditions since it is buried from the solvent.

4.5. A molecular explanation for the titration behavior of PDZ3 folding and misfolding

The biophysical analysis described here has led us to conclude that the intermediate species developed by PDZ3 upon unfolding are substantially different under neutral and acidic pH (≤ 3) conditions. Thus, the equilibrium experiments showed a net energetic destabilization of the trimeric species seen at neutral pH, which persisted as monomers during misfolding at pH ≤ 3. In addition, the non-fluorescent character when using ThT and ANS probes suggests that the intermediate structure at acidic pH is more compact than that at neutral pH and displays a lesser hydrophobic content to the solvent.

A β-aggregation propensity analysis of the PDZ3 X-ray structures by means of the Tango algorithm [30] did not reveal any substantial differences between pH 7.5 and pH 3, residues 340-350 (pertaining to β3 and α1 secondary structures) and 392-397 (deriving from β5 and α3) being the most prone to β-aggregation (Fig. S3). An inspection of PDZ3 X-ray structures shows that residues E334 from β3, and E396 and E401 from α3 may generate some electrostatic repulsion upon proton release at pH ≥ 3.5 [quantified as 40 $kJ \cdot mol^{-1}$ according to DSC unfolding experiments (Fig. 2)] and thus cause the neighbouring residues from the β3-α1 and β5-α3 regions to protrude from the protein leaving them susceptible to β-aggregation (Figs 7 and S3). These partly unfolded intermediates stabilized themselves through oligomerization in the trimeric species seen at neutral pH. Nevertheless, at pH ≤ 3 the protonated Glu residues did not develop such repellent electrostatic forces and the regions prone to aggregation did not protrude from PDZ3, which remained as a monomer in the solution. The 4.7 nm particles might arise from a non-specific aggregation of monomers, as has been shown in other examples [19]. These features may also explain the absence of fluorescence in the acidic particles and the highly fluorescent nature of those at neutral pH.

In support of these arguments it should be pointed out that the flipping of the α3 helix has been observed by other authors in hydrogen-exchange NMR experiments [29] and that we ourselves have described the structural interconnection between the α3 helix and the loop connecting the β2 and β3 strands [7]. Furthermore, as mentioned above, the α3 structural element has been proven to be a regulatory element of PDZ3 binding capacity [8] and is also an extra structural element of PDZ3, as compared to other PDZ topologies. Thus we may conclude that the C-terminal α3 helix also appears to be a regulatory element in the folding and assembling of the PDZ3 domain. In support of these conclusions we can point to the essentially different physico-chemical nature of the residues involved in the stacking of the α3 helix (mainly the above-mentioned Glu and aromatic residues) from those of the rest of the secondary structural elements, in which a collection of methyl-methyl mediated hydrophobic interactions, involving mainly aliphatic side-chains, can be found [31].

It must be pointed out that these electrostatic interactions between the α3 helix and the β2-β3 loop residues are almost certainly ultimately responsible for the reversible formation of the annular structures seen at pH 7.5 (Fig. 3) [4]. Further research is needed into this point to clarify whether such annular arrangements can cause toxicity *in vivo*, as has been shown in

some other examples [6,32,33]. Less is known about the molecular mechanism by which they are formed from PDZ3 trimers or about the hypothetical biological relevance of these supramacromolecular assemblies within the context of the *"*hub*"* protein PDS95, a member of the MAGUK family, the function of which has been described as a recruitment centre for proteins at the inner face of the neuron membrane [34,35]. Within this context, the electrostatics of the PDZ3 module might be modulated by the membrane micro-environment [24-28] to control, for instance, the spatial- and time-dependent release (as hub proteins do) of protein ligands via a conformational change in the α3 helix [8]. A similar distribution of charged and aromatic groups can be seen at the α3 helix in the PDZ3 module of the homologous DLG-2 protein from *drosophila* (PDB: 1PDR). Structural modelling has also begun to point to some possibility of a functional role for the linker sequence connecting PDZ1 and PDZ2 in PSD95, as well as a regulatory role for other linker segments in PSD95 [36-38].

Acknowledgements

This work was financed by grants CVI-05915 and CVI-05063 from the Andalucian Regional Government and BIO2009-13261-C02-01/02 from the Spanish Ministry of Science and Education. J.M.C. is a Spanish Government PhD fellow. E.S.C. was funded by a contract provided by the University of Granada. We thank our colleague Dr. Jon Trout for revising and correcting our English text.

References

[1] Frieden, C. Protein aggregation processes: In search of the mechanism. Protein Sci 16 (2007) 2334-2344.

[2] Pappu, R. V., X. Wang, A. Vitalis, and S. L. Crick A polymer physics perspective on driving forces and mechanisms for protein aggregation. Arch Biochem Biophys 469 (2008) 132-141.

[3] Knowles, T. P., C. A. Waudby, G. L. Devlin, S. I. Cohen, A. Aguzzi, M. Vendruscolo, E. M. Terentjev, M. E. Welland, and C. M. Dobson An analytical solution to the kinetics of breakable filament assembly. Science 326 (2009) 1533-1537.

[4] Murciano-Calles, J., E. S. Cobos, P. L. Mateo, A. Camara-Artigas, and J. C. Martinez An oligomeric equilibrium intermediate as the precursory nucleus of globular and fibrillar supramacromolecular assemblies in a PDZ domain. Biophys J 99 (2010) 263-272.

[5] Lansbury, P. T. and H. A. Lashuel A century-old debate on protein aggregation and neurodegeneration enters the clinic. Nature 443 (2006) 774-779.

[6] Jang, H., J. Zheng, R. Lal, and R. Nussinov New structures help the modeling of toxic amyloidbeta ion channels. Trends Biochem Sci 33 (2008) 91-100.

[7] Camara-Artigas, A., J. Murciano-Calles, J. A. Gavira, E. S. Cobos, and J. C. Martinez Novel conformational aspects of the third PDZ domain of the neuronal post-synaptic

density-95 protein revealed from two 1.4A X-ray structures. J Struct Biol 170 (2010) 565-569.

[8] Petit, C. M., J. Zhang, P. J. Sapienza, E. J. Fuentes, and A. L. Lee Hidden dynamic allostery in a PDZ domain. Proc Natl Acad Sci U S A 106 (2009) 18249-18254.

[9] Gill, S. C. and P. H. von Hippel Calculation of protein extinction coefficients from amino acid sequence data. Anal Biochem 182 (1989) 319-326.

[10] Viguera, A. R., J. C. Martinez, V. V. Filimonov, P. L. Mateo, and L. Serrano Thermodynamic and kinetic analysis of the SH3 domain of spectrin shows a two-state folding transition. Biochemistry 33 (1994) 2142-2150.

[11] Cobos, E. S., M. T. Pisabarro, M. C. Vega, E. Lacroix, L. Serrano, J. Ruiz-Sanz, and J. C. Martinez A miniprotein scaffold used to assemble the polyproline II binding epitope recognized by SH3 domains. J Mol Biol 342 (2004) 355-365.

[12] Martinez, J. C., M. el Harrous, V. V. Filimonov, P. L. Mateo, and A. R. Fersht A calorimetric study of the thermal stability of barnase and its interaction with 3'GMP. Biochemistry 33 (1994) 3919-3926.

[13] Fu, L. and E. Freire On the origin of the enthalpy and entropy convergence temperatures in protein folding. Proc Natl Acad Sci U S A 89 (1992) 9335-9338.

[14] Baldwin, R. L. and N. Muller Relation between the convergence temperatures Th* and Ts* in protein unfolding. Proc Natl Acad Sci U S A 89 (1992) 7110-7113.

[15] Privalov, P. L. Stability of proteins. Proteins which do not present a single cooperative system. Adv Protein Chem 35 (1982) 1-104.

[16] Ragone, R. and G. Colonna Enthalpy-entropy balance and convergence temperatures in protein unfolding. J Biol Chem 269 (1994) 4047-4049.

[17] Harper, J. D. and P. T. Lansbury, Jr. Models of amyloid seeding in Alzheimer's disease and scrapie: mechanistic truths and physiological consequences of the time-dependent solubility of amyloid proteins. Annu Rev Biochem 66 (1997) 385-407.

[18] Kad, N. M., S. L. Myers, D. P. Smith, D. A. Smith, S. E. Radford, and N. H. Thomson Hierarchical assembly of beta2-microglobulin amyloid in vitro revealed by atomic force microscopy. J Mol Biol 330 (2003) 785-797.

[19] Smith, A. M., T. R. Jahn, A. E. Ashcroft, and S. E. Radford Direct observation of oligomeric species formed in the early stages of amyloid fibril formation using electrospray ionisation mass spectrometry. J Mol Biol 364 (2006) 9-19.

[20] Kardos, J., K. Yamamoto, K. Hasegawa, H. Naiki, and Y. Goto Direct measurement of the thermodynamic parameters of amyloid formation by isothermal titration calorimetry. J Biol Chem 279 (2004) 55308-55314.

[21] Jeppesen, M. D., P. Westh, and D. E. Otzen The role of protonation in protein fibrillation. FEBS Lett 584 (2010) 780-784.

[22] Gerber, R., A. Tahiri-Alaoui, P. J. Hore, and W. James Conformational pH dependence of intermediate states during oligomerization of the human prion protein. Protein Sci 17 (2008) 537-544.

[23] Juarez, J., S. G. Lopez, A. Cambon, P. Taboada, and V. Mosquera Influence of electrostatic interactions on the fibrillation process of human serum albumin. J Phys Chem B 113 (2009) 10521-10529.

[24] Lockhart, D. J. and P. S. Kim Electrostatic screening of charge and dipole interactions with the helix backbone. Science 260 (1993) 198-202.

[25] Ma, J. C. and D. A. Dougherty The Cationminus signpi Interaction. Chem Rev 97 (1997) 1303-1324.

[26] Lund, M. and B. Jonsson On the charge regulation of proteins. Biochemistry 44 (2005) 5722-5727.

[27] Berry, B. W., M. M. Elvekrog, and C. Tommos Environmental modulation of protein cation-pi interactions. J Am Chem Soc 129 (2007) 5308-5309.

[28] Wu, R. and T. B. McMahon Investigation of cation-pi interactions in biological systems. J Am Chem Soc 130 (2008) 12554-12555.

[29] Feng, H., N. D. Vu, and Y. Bai Detection of a hidden folding intermediate of the third domain of PDZ. J Mol Biol 346 (2005) 345-353.

[30] Fernandez-Escamilla, A. M., F. Rousseau, J. Schymkowitz, and L. Serrano Prediction of sequence-dependent and mutational effects on the aggregation of peptides and proteins. Nat Biotechnol 22 (2004) 1302-1306.

[31] Gianni, S., T. Walma, A. Arcovito, N. Calosci, A. Bellelli, A. Engstrom, C. Travaglini-Allocatelli, M. Brunori, P. Jemth, and G. W. Vuister Demonstration of long-range interactions in a PDZ domain by NMR, kinetics, and protein engineering. Structure 14 (2006) 1801-1809.

[32] Shirwany, N. A., D. Payette, J. Xie, and Q. Guo The amyloid beta ion channel hypothesis of Alzheimer's disease. Neuropsychiatr Dis Treat 3 (2007) 597-612.

[33] Lashuel, H. A. and P. T. Lansbury, Jr. Are amyloid diseases caused by protein aggregates that mimic bacterial pore-forming toxins? Q Rev Biophys 39 (2006) 167-201.

[34] Kim, E. and M. Sheng PDZ domain proteins of synapses. Nat Rev Neurosci 5 (2004) 771-781.

[35] Feng, W. and M. Zhang Organization and dynamics of PDZ-domain-related supramodules in the postsynaptic density. Nat Rev Neurosci 10 (2009) 87-99.

[36] Long, J. F., H. Tochio, P. Wang, J. S. Fan, C. Sala, M. Niethammer, M. Sheng, and M. Zhang Supramodular structure and synergistic target binding of the N-terminal tandem PDZ domains of PSD-95. J Mol Biol 327 (2003) 203-214.

[37] Korkin, D., F. P. Davis, F. Alber, T. Luong, M. Y. Shen, V. Lucic, M. B. Kennedy, and A. Sali Structural modeling of protein interactions by analogy: application to PSD-95. PLoS Comput Biol 2 (2006) e153.

[38] Wang, W., J. Weng, X. Zhang, M. Liu, and M. Zhang Creating conformational entropy by increasing interdomain mobility in ligand binding regulation: a revisit to N-terminal tandem PDZ domains of PSD-95. J Am Chem Soc 131 (2009) 787-796.

[39] Dolinsky, T. J., P. Czodrowski, H. Li, J. E. Nielsen, J. H. Jensen, G. Klebe, and N. A. Baker PDB2PQR: expanding and upgrading automated preparation of biomolecular structures for molecular simulations. Nucleic Acids Res 35 (2007) W522-525.

Figure Captions

Figure 1. Calorimetric traces of PDZ3. The experiments were carried out at a protein concentration of 1.5 mg·mL^{-1} and obtained at different pH values (gray symbols). Their best fittings to the respective equilibrium models are also shown (solid black lines).

Figure 2. Analysis of the electrostatic contribution of Glu and Asp residues to the unfolding enthalpy of PDZ3. The linear correlation among enthalpies derived from two-state analyses (circles) is represented by a solid line. Dashed gray lines represent the 95 % confidence intervals of this linear regression. Gray squares with error bars are the enthalpy values for three-state analyses. The diamond represents the convergence value of 54 J·g^{-1} at 110 ºC for small globular proteins.

Figure 3. A representation of the most salient features of PDZ3 misfolding under neutral and acidic pH conditions.

Figure 4. The DLS distribution of hydrodynamic species of PDZ3 at pH 3. A protein solution at a concentration of 8 mg·mL^{-1} was heated to 60 ºC, at which point the mass evolution of the species as a function of incubation time (in gray) was recorded.

Figure 5. TEM analysis of PDZ3 supramacromolecular assemblies at pH 3. The left panel shows the 4.7 nm particles, seen also by DLS, after 4 hours' incubation of an 8 mg·mL^{-1} sample at 60 ºC. The fibrils organized after 1 and 7 days' incubation are shown in the centre and right panels respectively. The scale bar corresponds to 200 nm.

Figure 6. Growth kinetics of ThT and ANS fluorescence emission. An 8 mg·mL-1 PDZ3 sample was incubated in the presence of 12 μM of ThT or 20 μM ANS at pH 3. Time dependence of the fluorescence signal versus incubation time at 60 ºC for ThT (panel A) and ANS (panel B).

Figure 7. Electrostatic surface of the PDZ3 domain calculated with APBS [39] implemented in PyMOL (DeLano Scientific Palo Alto, CA; *www.pymol.org*).A detail of the interface of the α3 helix at the C-terminus of PDZ3 with the β2-β3 loop showing the spatial arrangement of

Phe, Tyr and Glu residues is shown. The green dashed lines represent relative distances between residues.

Table 1. Thermodynamic parameters for the unfolding of the PDZ3 domain of PSD95 obtained from fittings to N⇄U and 3N⇄3U⇄I_3 models [*]

pH	T_{N-U} (ºC)	$\Delta H_{N-U}(T_{N-U})$ (kJ·mol^{-1})	T_{U-In} (ºC)	$\Delta H_{U-In}(T_{U-In})$ (kJ·mol^{-1})	$\Delta G_{N-U}(298)$ (kJ·mol^{-1})	R^2
			3N ⇄ 3U ⇄ I_3			
7.5	70.4 ± 0.5	335 ± 20	79.2 ± 1.2	-130 ± 10	39 ± 6	0.996
4.0	70.0 ± 0.3	335 ± 10	89.3 ± 1.4	-145 ± 30	33 ± 8	0.983
3.5	67.4 ± 0.2	340 ± 10	77.0 ± 1.7	-110 ± 20	37 ± 7	0.999
			N ⇄ U			
3.0	59.0 ± 0.1	325 ± 5	-	-	26 ± 2	0.999
2.5	51.6 ± 0.1	280 ± 5	-	-	17 ± 2	0.998
2.0	47.5 ± 0.1	265 ± 5	-	-	14 ± 2	0.998

[*] The unfolding values at pH 7.5 were obtained from a previous work [4]. For the remaining pH values the protein concentration was 1.5 mg·mL^{-1}. The error intervals for the three-state parameters were estimated by comparing the values obtained when n = 3 and 4. The errors in two-state analyses were taken to be three times the fitting standard errors (99 % confidence).

Figure 1

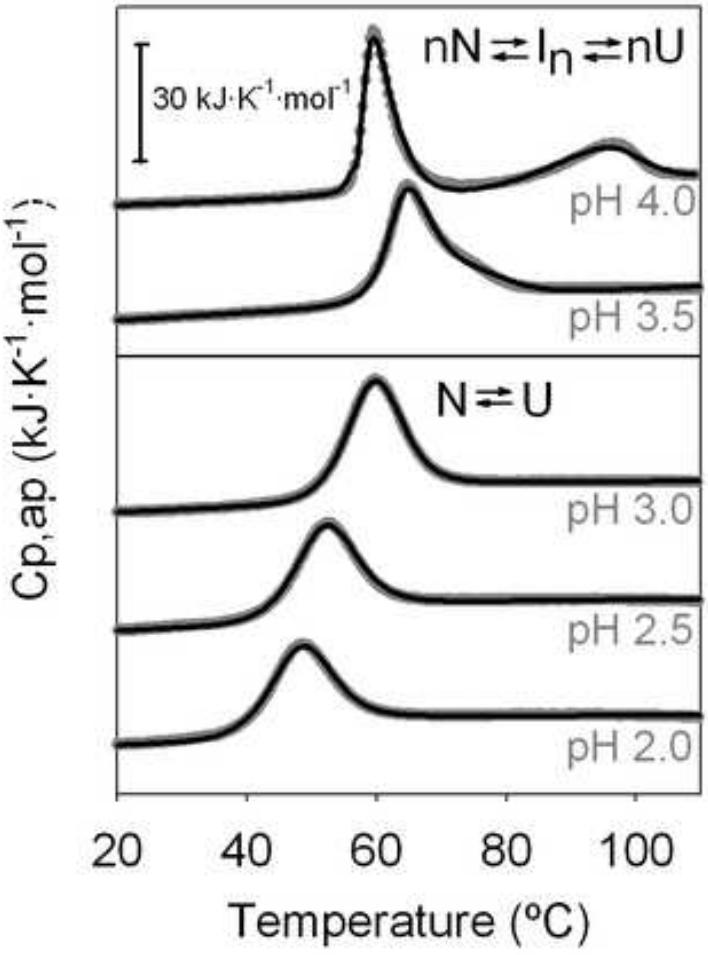

Figure 2

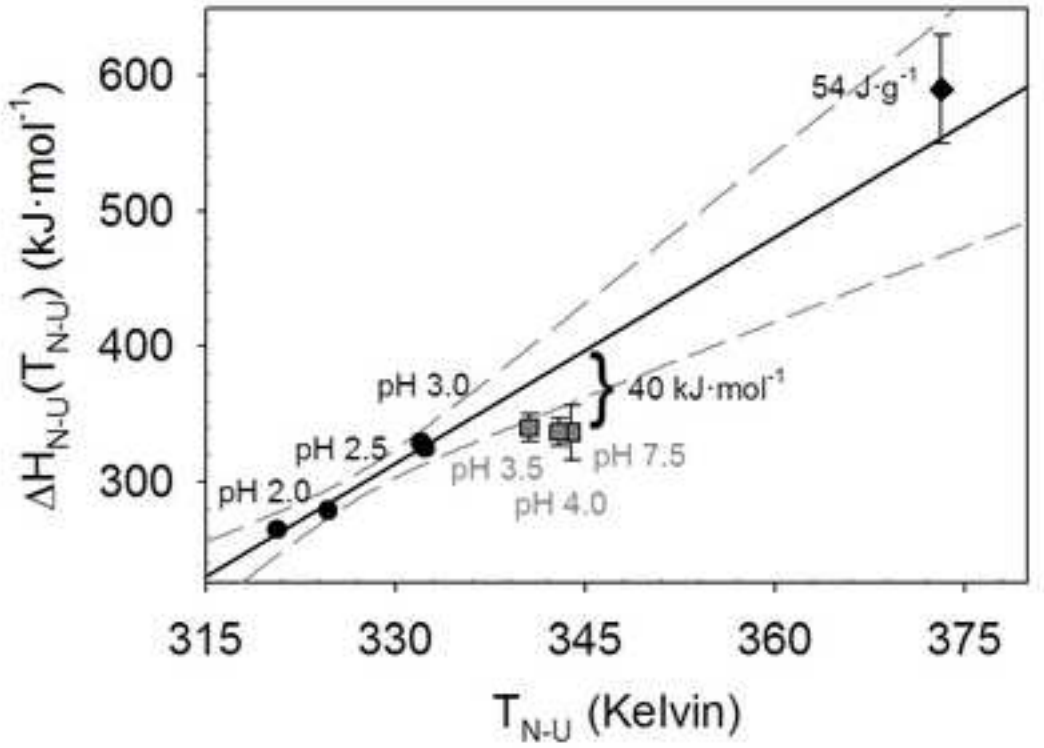

Figure 3

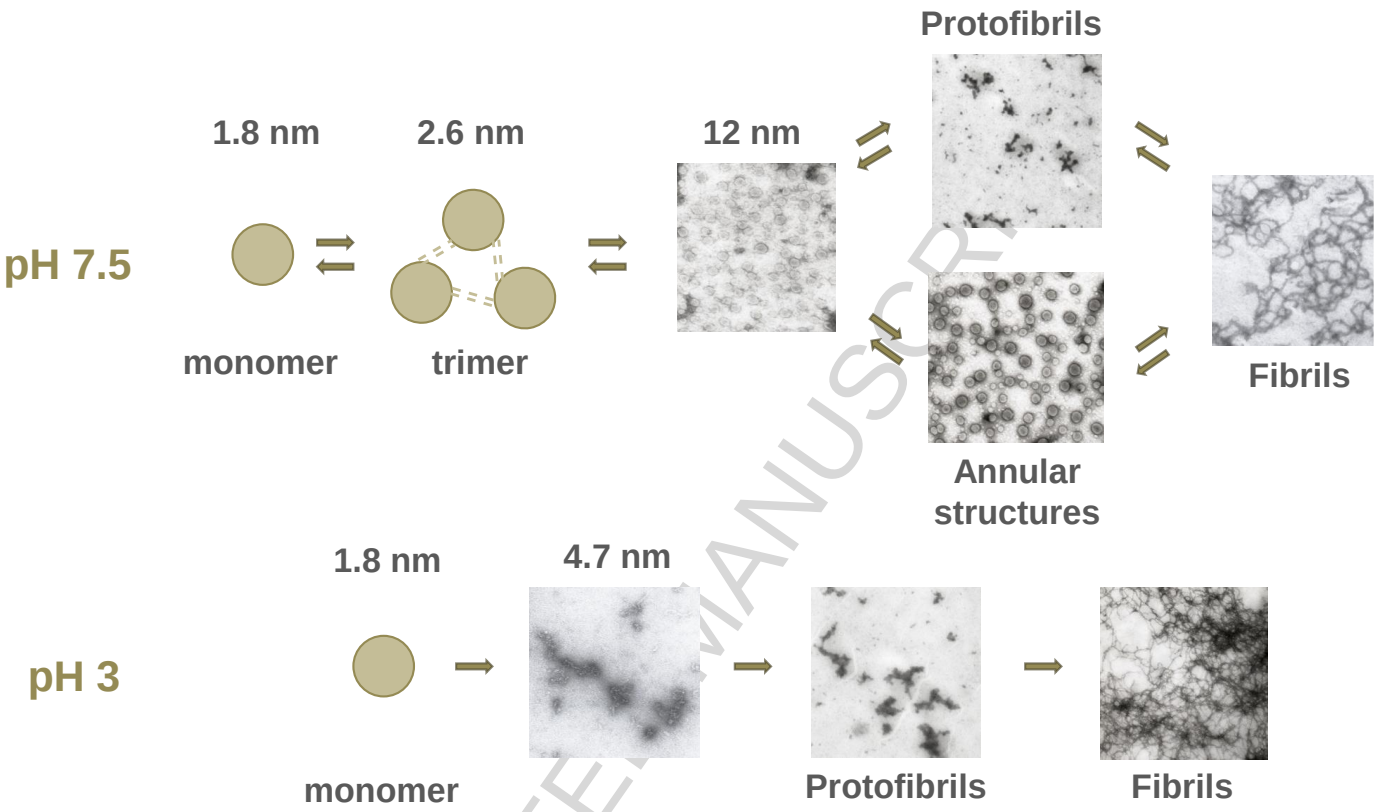

Figure 4

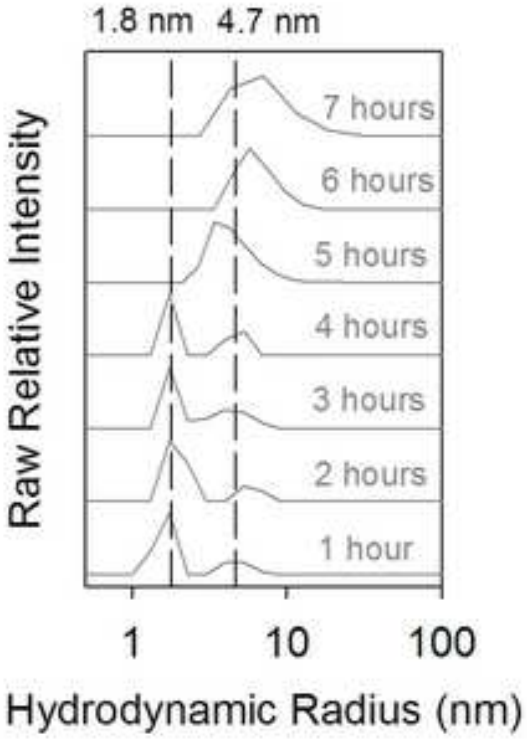

Figure 5

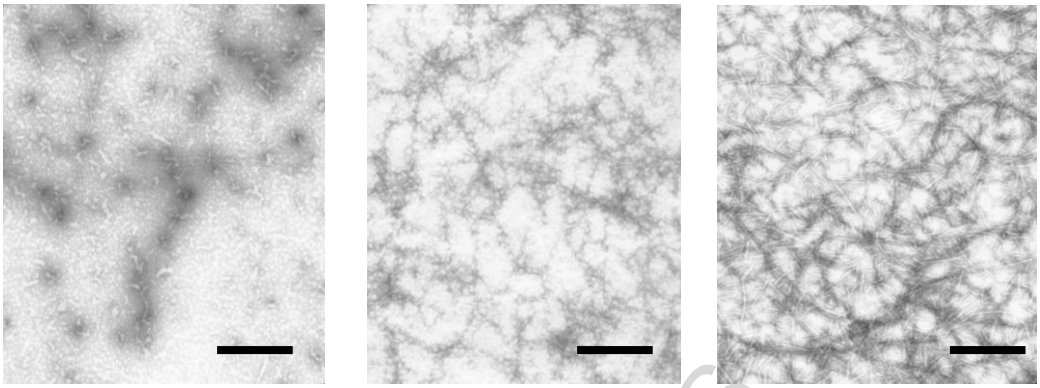

4 hours 1 day 7 days

Figure 6

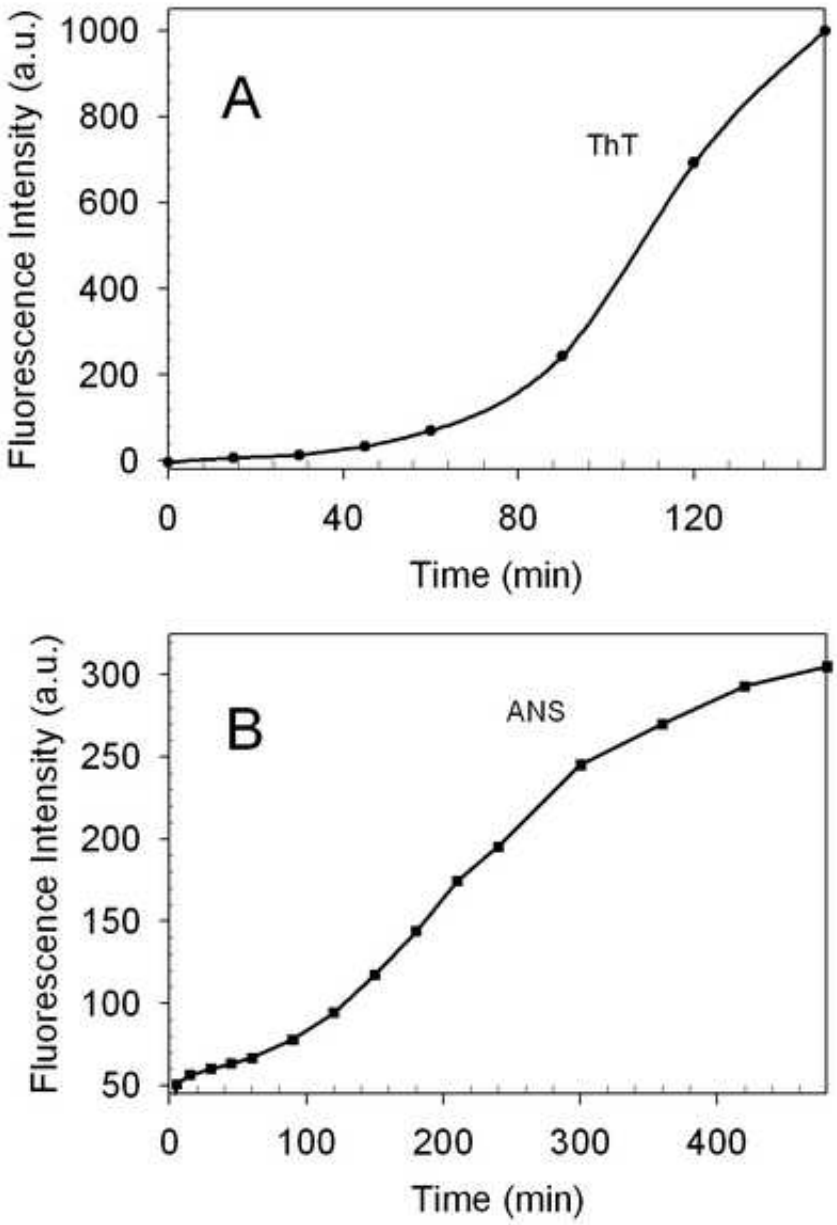

Figure 7

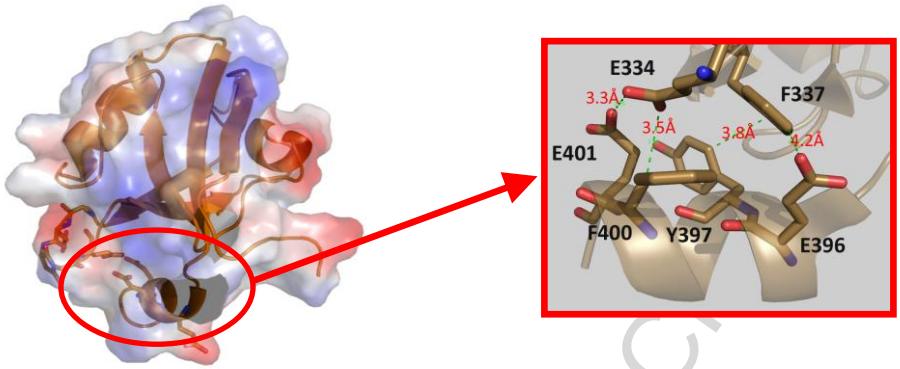

Graphical abstract